Supplementary Figures for

Directional transition from initiation to elongation in bacterial translation

Akanksha Goyal[1], Riccardo Belardinelli[1], Cristina Maracci[1], Pohl Milón[1,2] and Marina V. Rodnina[1,*]

[1] Department of Physical Biochemistry, Max Planck Institute for Biophysical Chemistry, 37077 Göttingen, Germany

[2] Present address: School of Medicine, Faculty of Health Sciences, Universidad Peruana de Ciencias Aplicadas - UPC, Lima, L-33, Perú

* To whom correspondence should be addressed. Tel: +49 551 201 2900; Fax: +49 551 2905; Email: rodnina@mpibpc.mpg.de

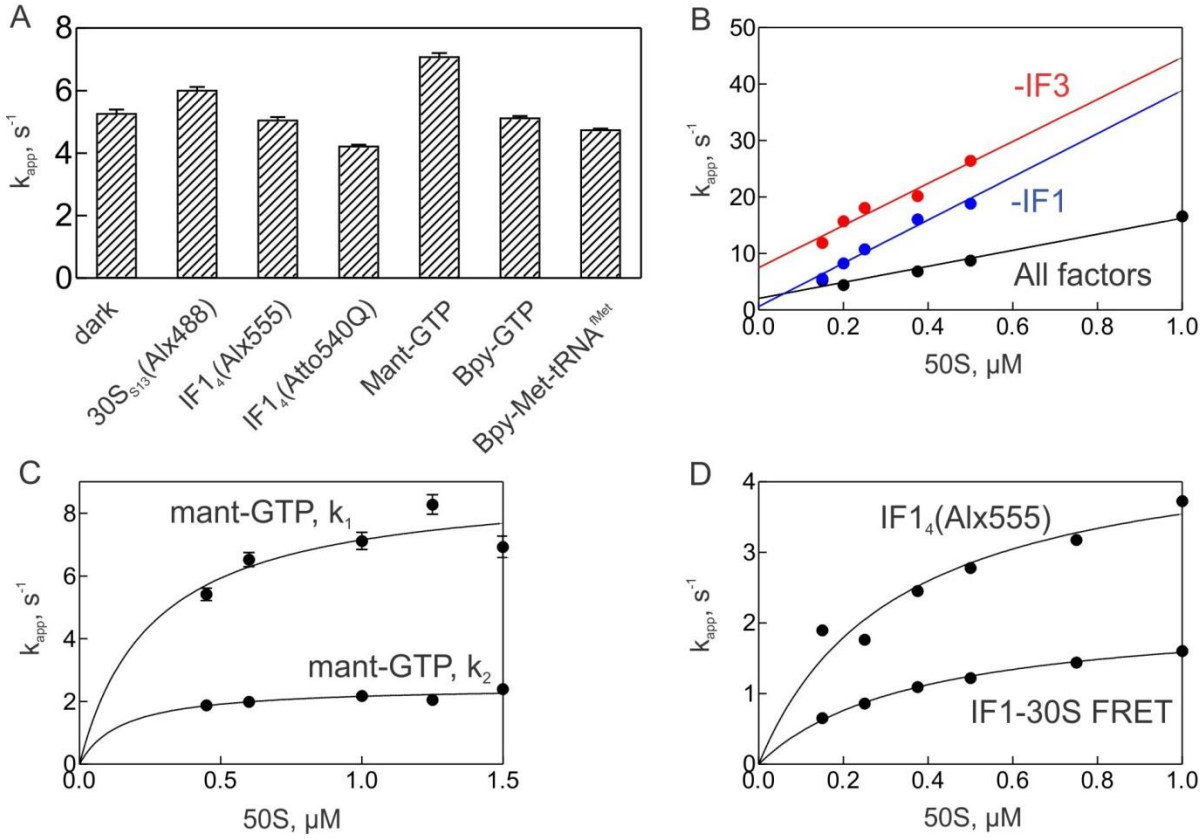

Supplementary Figure S1. Apparent rates of reactions during 70S IC maturation. 30S IC formed in the presence of different fluorescence-labeled initiation components was rapidly mixed with 50S subunits in a stopped-flow machine. Apparent rate constants were derived from double exponential fitting of time courses. A. Apparent rates of LS (30S IC (0.05 μM); 50S (0.25 μM)) in the presence of different reporters. B. Concentration dependence of k_{app} values of LS. In A and B, the k_{app} value of the predominant phase (>65% of total amplitude change) is reported. The k_{app} value for the minor phase was <1 s^{-1} and was concentration-independent (not shown). C. Concentration dependence of k_{app} values of biphasic FRET change between mant-GTP and Trp residue of IF2. D. Concentration dependence of k_{app} values of the predominant phase of fluorescence change of IF1$_4$(Alx555) (83% of total amplitude change) and FRET change between IF1$_4$(Atto540Q) and 30S$_{S13}$(Alx488) (73% of total amplitude change). The k_{app} value for the minor phase was <0.5 s^{-1}. Values are mean ± s.e.m of exponential fitting of 7-10 time courses taken for averaging.

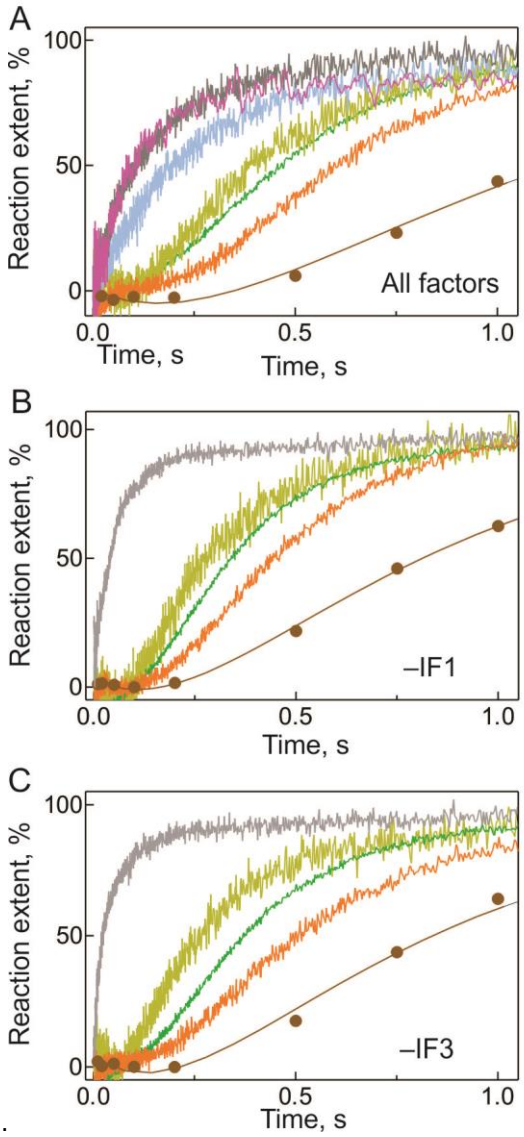

Supplementary Figure S2. Direct comparison of reaction time courses during 70S IC maturation. Presented are time courses at 1 µM 50S subunit concentration. 50S subunit association with the 30S IC (grey), GTPase activation (monitored with mant-GTPγS, pink), and changes in IF1 environment (light blue) follow exponential kinetics. All other reactions, such as Pi release (gold), tRNA release from IF2 (green), GDP release (orange) and peptide bond formation (brown) are preceded by a delay phase. All traces were normalized with respect to amplitude changes to facilitate visual comparison of time courses. The reactions were monitored in the presence of (A) all factors, or (B) in the absence of IF1, or (C) in the absence of IF3. GTPase activation (smoothened using GraphPad prism software) and the change in IF1 environment are shown only for the full complex; multiphasic observables such as FRET between mant-GTP and IF2, as well as FRET between $IF1_4$(Atto540Q) and $30S_{S13}$(Alx488) are not shown for visual clarity.

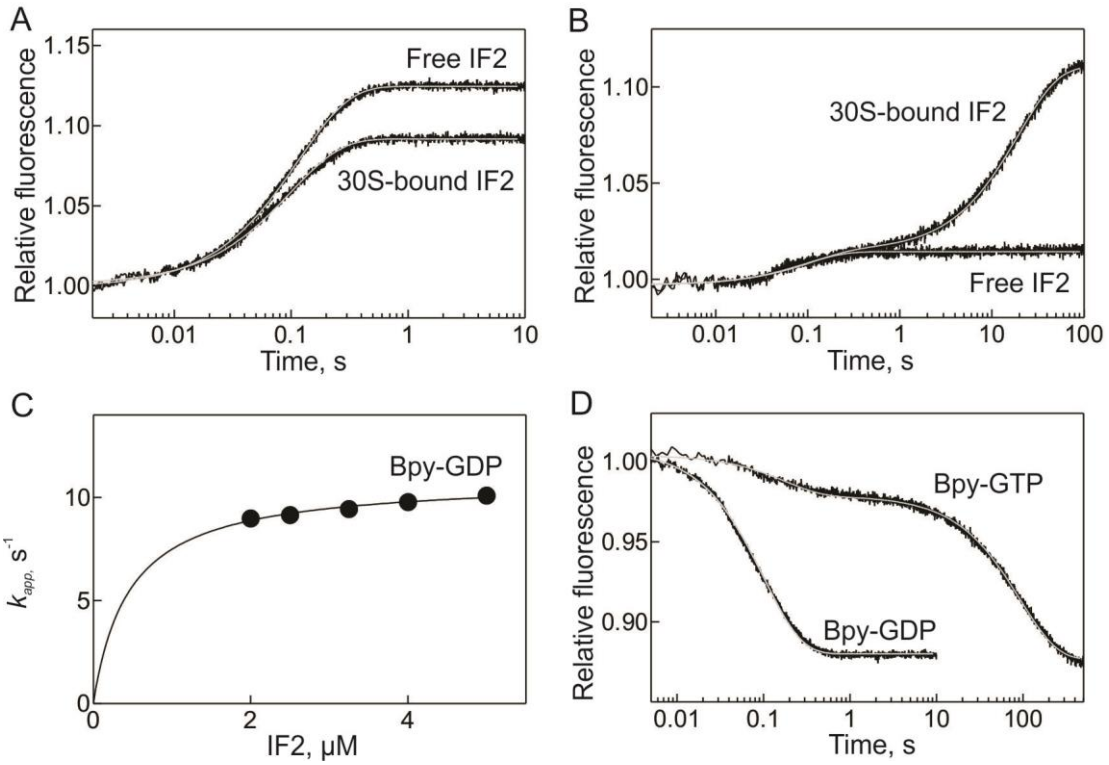

Supplementary Figure S3. Binding and dissociation kinetics of Bpy-GTP and Bpy-GDP. Indicated components were rapidly mixed in a stopped-flow apparatus and the fluorescence changes of the Bpy-labeled guanine nucleotide were monitored. A. Time courses of Bpy fluorescence change upon binding of Bpy-GDP (2 μM) to free IF2 (0.1 μM) or IF2 bound to 30S PIC (0.1 μM) (formed in the absence of any nucleotide). The rate determined from the single-exponential fitting of time courses (smooth lines) was 9 ± 1 s^{-1}, in both cases. B. Time courses of Bpy fluorescence change upon binding of Bpy-GTP (2 μM) to free IF2 (0.1 μM) or IF2 bound to 30S PIC (0.1 μM). Upon binding of Bpy-GTP to IF2 on the 30S IC, the fluorescence increase is biphasic with a rapid step (9 ± 1 s^{-1}) with a very small amplitude (15% of the total amplitude change), and a slow phase (0.05 ± 0.002 s^{-1}) accounting for the remaining amplitude change. Binding of Bpy-GTP to free IF2 displayed only the first small phase, which occurred at the rate of 10 s^{-1} (similar to Bpy-GDP), indicating that this phase may arise from a conformational rearrangement that is common to the binding of both nucleotides to IF2. C. Concentration dependence of k_{app} values of Bpy-GDP binding to free IF2 upon mixing of the nucleotide (2 μM) with increasing concentrations of free IF2. The k_{app} saturated at high IF2 concentrations (10 ± 1 s^{-1}) indicative of a monomolecular rearrangement which follows the binding step. The k_{app} are derived from single-exponential fitting of time courses and represent the mean ± s.e.m. D. Time courses of Bpy-GTP or Bpy-GDP release from IF2 bound to the 30S IC, upon chase with 125-fold excess of non-fluorescent GTP. The dissociation rate constants determined from the chase experiments were 10 s^{-1} for Bpy-GDP (one-exponential fitting) and predominantly (80% of the reaction amplitude) 0.01 s^{-1} for Bpy-GTP (two-exponential fitting).

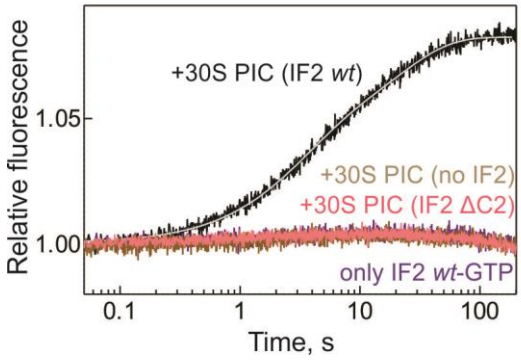

Supplementary Figure S4. Kinetics of Bpy-Met-tRNA^{fMet} binding to IF2 on the 30S IC. 30S PIC lacking fMet-tRNA^{fMet} (0.1 μM) was rapidly mixed with Bpy-Met-tRNA^{fMet} (0.3 μM) at 37°C in a stopped-flow machine. The fluorescence changes of Bpy-Met-tRNA^{fMet} were monitored with time. The time course of Bpy-Met-tRNA^{fMet} recruitment to 30S PIC by IF2 *wild-type* (*wt*) showed biphasic kinetics and was fit with a double-exponential function. Both phases were equal in amplitude and had the rates 0.35 s^{-1} and 0.05 s^{-1}, respectively.

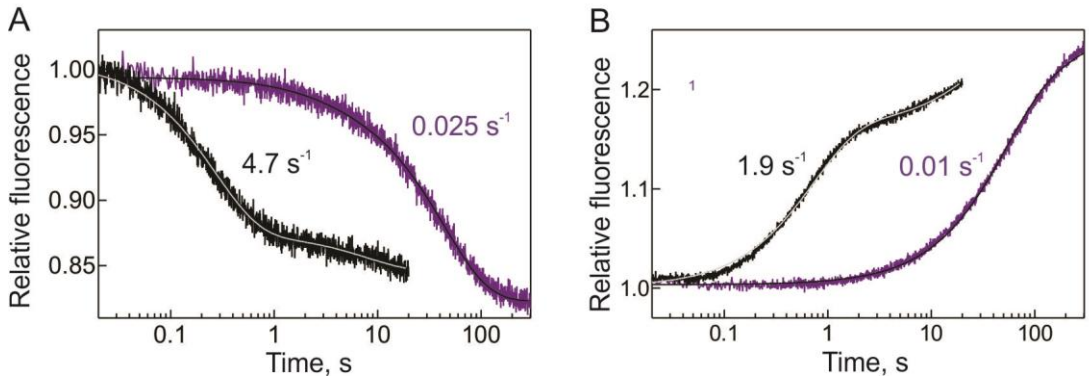

Supplementary Figure S5. Release of IF1 from the 30SIC. 30S IC (0.05 μM) formed with (A) $IF1_4$(Alx555) or (B) $30S_{S13}$(Alx488) and $IF1_4$(Atto540Q), was rapidly mixed in a stopped-flow machine, with 50S subunits (1 μM, black) or a 20-fold excess of non-fluorescent IF1 (1 μM, purple). The time courses were fitted with a double-exponential function. The k_{app} of the predominant phase (>65% of total amplitude change) is shown.

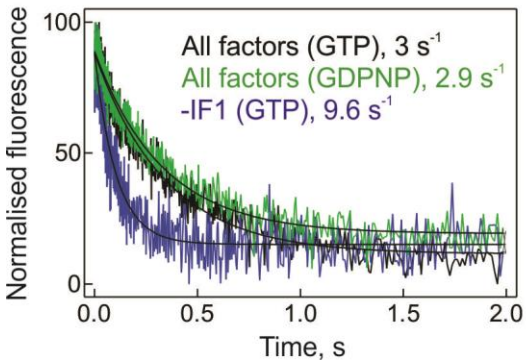

Supplemental Figure S6. Dissociation of IF3 from the 70S IC. 30S ICs were rapidly mixed with 50S subunits (1 μM) in a stopped-flow machine and time courses of IF3 dissociation (measured by loss of FRET between fluorescein-labeled fMet-tRNA^{fMet} and IF3$_{166}$(Alx555)) were monitored. Rates derived from single-exponential fitting of time courses are shown.

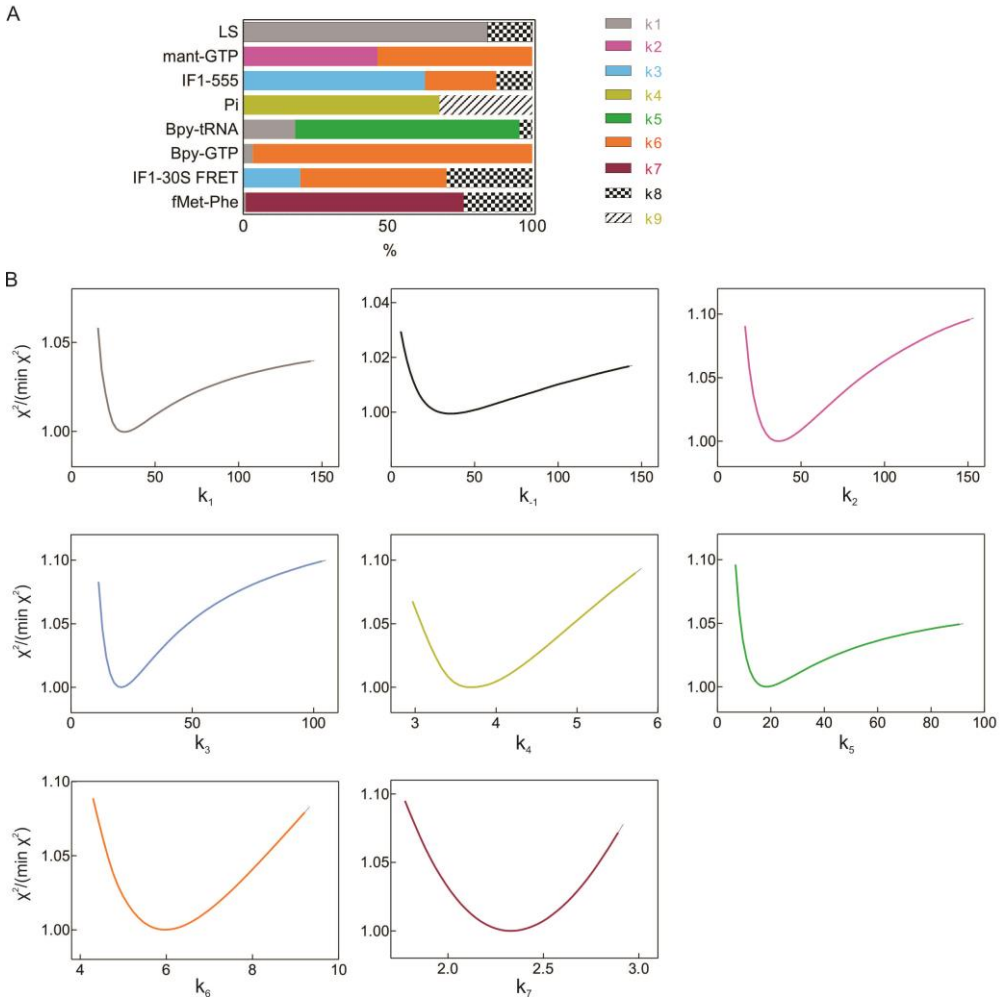

Supplementary Figure S7. Statistical analysis of global fitting of datasets using KinTek Explorer. Time courses of all observables (LS; FRET between mant-GTP and Trp residue of IF2; fluorescence changes of $IF1_4$(Alx555); Pi release; fluorescence changes of Bpy-Met-$tRNA^{fMet}$; fluorescence changes of Bpy-GTP; and dequenching of $30S_{S13}$(Alx488) by $IF1_4$(Atto540Q)) were obtained at increasing concentrations of 50S subunits, and collectively evaluated by numerical integration using a 9-step kinetic model (see Results). Amplitudes are presented as % of fluorescence change at a given step compared to the total fluorescence change. For all observables where the fluorescence changes go into one direction, the total amplitude is set at 1-100%. For mant-GTP, where the fluorescence change has an upward and downward phase, the amplitudes of both steps were summed up, disregarding the sign. A. Distribution of amplitudes of the observables along different steps of the model. B. Global minima and confidence intervals of elemental rate constants (s^{-1}) derived from global fitting of datasets.

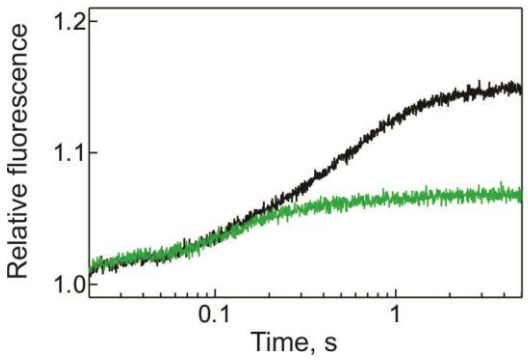

Supplementary Figure S8. IF1 release from 70S IC formed with IF2ΔN. 30S IC, formed with the IF2ΔN variant and GTP (black) or GTPγS (green), was rapidly mixed with 50S subunits (1 μM) in the stopped-flow apparatus. The time courses of IF1 dissociation were monitored via FRET between $30S_{S13}$(Alx488) and $IF1_4$(Atto540Q).